Spin transfer from dark matter to gas during halo formation

Jie Li,[1⋆] Danail Obreschkow,[1,2] Chris Power,[1,2] and Claudia del P. Lagos[1,2]
[1] *International Centre for Radio Astronomy Research, M468, University of Western Australia, 35 Stirling Hwy, Perth, WA 6009, Australia*
[2] *ARC Centre of Excellence for All Sky Astrophysics in 3 Dimensions (ASTRO 3D)*

Accepted XXX. Received YYY; in original form ZZZ

Introduction

Numerical studies show that many factors can affect the AM of galaxies, including

- stellar feedback (e.g. DeFelippis et al. 2017),
- gas accretion (e.g. El-Badry et al. 2018),
- galaxy mergers (e.g. Lagos et al. 2018b,a),
- along with the primordial spin of the pristine halo gas itself. (in the standard cold dark matter cosmological framework, protogalactic haloes of dark matter (DM) and diffuse gas acquire AM through tidal torques (e.g. Peebles 1969).)

In the protogalactic haloes, DM and gas share the same sAM?

- Zjupa & Springel (2017) found that specific AM (sAM) of the halo gas lies a factor 1.8 above that of the DM in the illustris simulation with full physics turned on. (merger & feedback)
- Even cosmological simulations of DM and an ideal gas, without radiative cooling and galaxy formation physics (Chen et al. 2003; Sharma & Steinmetz 2005; Zjupa & Springel 2017), consistently showed that the ratio between the mean spin parameters of gas and DM, which is equal to the ratio of the mean sAM, lies around 1.3–1.4 at redshift z = 0.

机制？

- Sharma et al. (2012) suggested that DM has an inside-out transfer of AM, due to dynamical friction, while gas has an outside-in transfer of AM, as the low AM gas in the inner parts shocks with high AM gas falling in from the outer parts. Then the outer part of the gas moves out of the virial radius as time progresses. (but FOF)

- Zjupa & Springel (2017) comment that gas continuously acquires sAM throughout cosmic time. This acquisition could be explained by mergers getting ram pressure stripped during halo infall, inducing a decoupling between gas and DM and producing torques between these two components as a consequence. This allows a net transfer of angular momentum from dark matter to gas. (but direction)

2 SPIN IN COSMOLOGICAL SIMULATIONS

$$\lambda = \frac{J|E|^{1/2}}{GM^{5/2}}, \tag{1}$$

$$\lambda' = \frac{j}{\sqrt{2}R_{\rm vir}V_{\rm vir}}, \tag{2}$$

z	$\langle\lambda'_{\rm tot}\rangle$	$\langle\lambda'_{\rm gas}\rangle$	$\langle\lambda'_{\rm DM}\rangle$	$\langle\lambda'_{\rm gas}\rangle/\langle\lambda'_{\rm DM}\rangle$
0	0.0305	0.0424	0.0293	1.44
1	0.0318	0.0425	0.0309	1.37
2	0.0305	0.0380	0.0301	1.26
3	0.0280	0.0331	0.0280	1.18
4	0.0253	0.0285	0.0255	1.11

Table 1. Spin parameter evolution of haloes in the SURFS simulation L210N1024NR. Column 1: the redshifts; Column 2: the mean value of spin parameter of haloes; Column 3: the mean value of spin parameter of gas; Column 4: the mean value of spin parameter of DM; Column 5: the ratio between mean spin parameter of gas to that of DM.

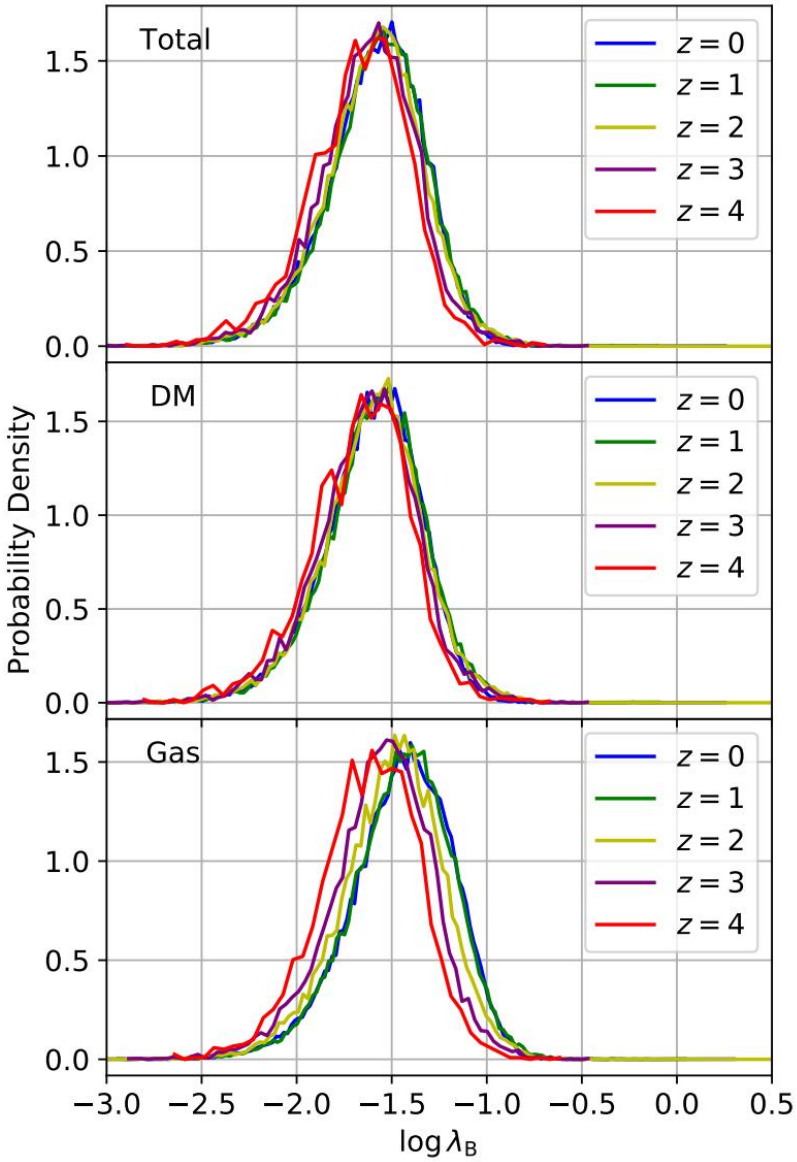

Figure 1. *Top panel:* Spin parameter distributions of all materials in haloes at different redshifts. *Middle panel:* Spin parameter distributions of DM in haloes at the same redshifts. *Bottom panel:* Spin parameter distributions of gas in haloes at the same redshifts.

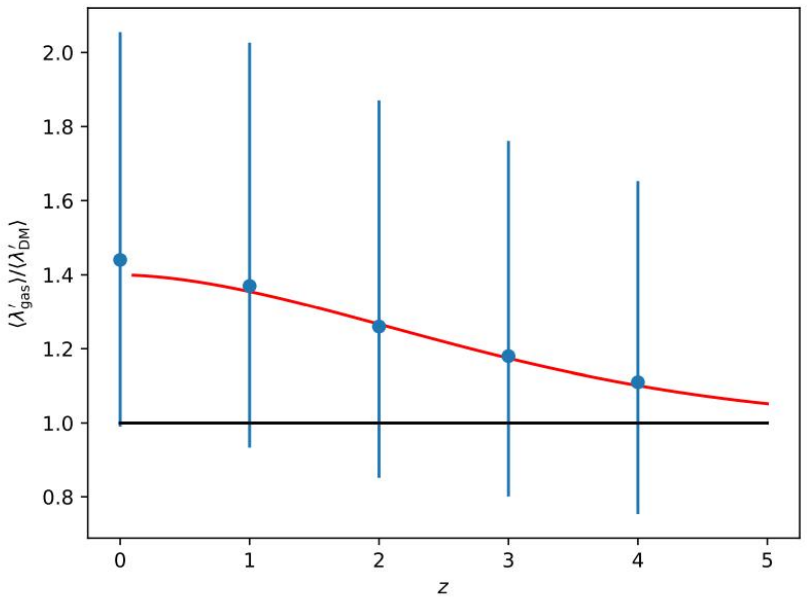

Figure 2. $z - \langle\lambda'_{\rm gas}\rangle/\langle\lambda'_{\rm DM}\rangle$ relation from SURFS. The blue points present the ratio of $\langle\lambda'_{\rm gas}\rangle/\langle\lambda'_{\rm DM}\rangle$ at different redshifts. Vertical bars represent the 16th to 84th quantile ranges of the individual $\lambda'_{\rm gas}/\lambda'_{\rm DM}$ values at each redshift. The red curve shows the fit of equation (3), which is asymptotes to unity (black line) at a high z.

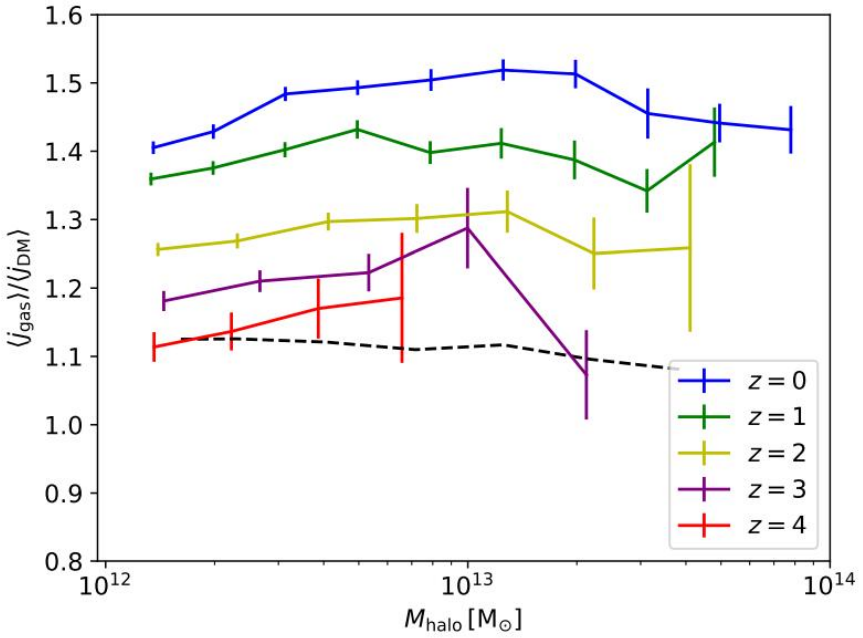

Figure 3. Halo mass-$j_{\rm gas}/j_{\rm DM}$ relation at different redshifts. The errorbars present the jacknife uncertainty of the mean value of each bin. Black dashed line shows the $j_{\rm gas}/j_{\rm DM}$ at the turnaround point $z_{\rm turn}$, which is discussed in Section 4.

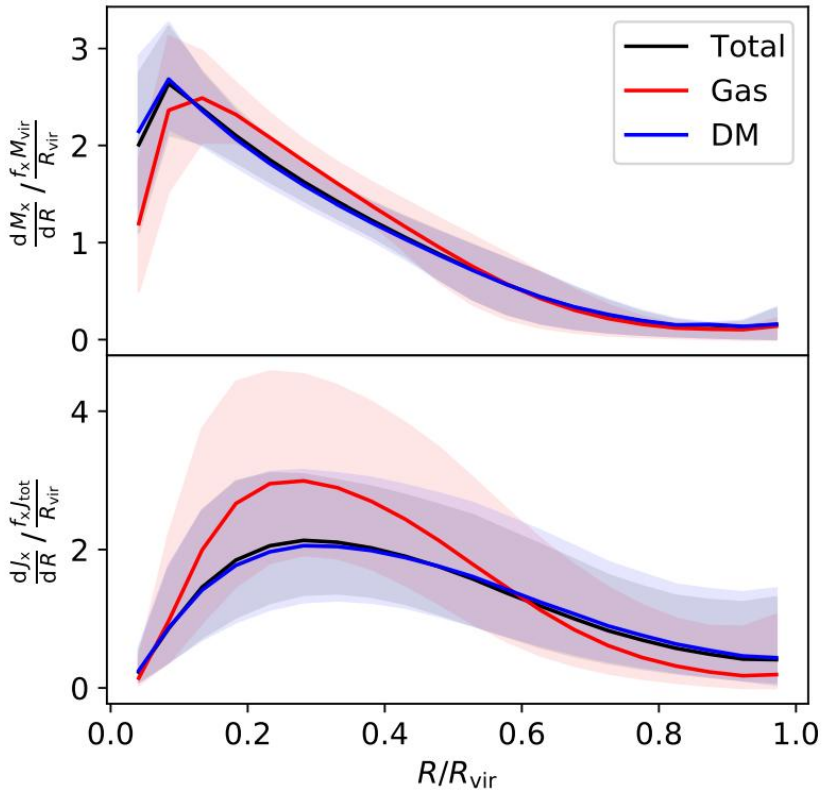

Figure 4. *Top panel*: Mass distribution of each component. The mass distributions of gas and DM are similar. Most of the mass concentrates on the inner halo. *Bottom panel*: AM distribution of each component. Gas has excess AM comparing with DM at $R < 0.6R_{\rm vir}$, larger than the excess AM of DM comparing with gas at $R > 0.6R_{\rm vir}$.

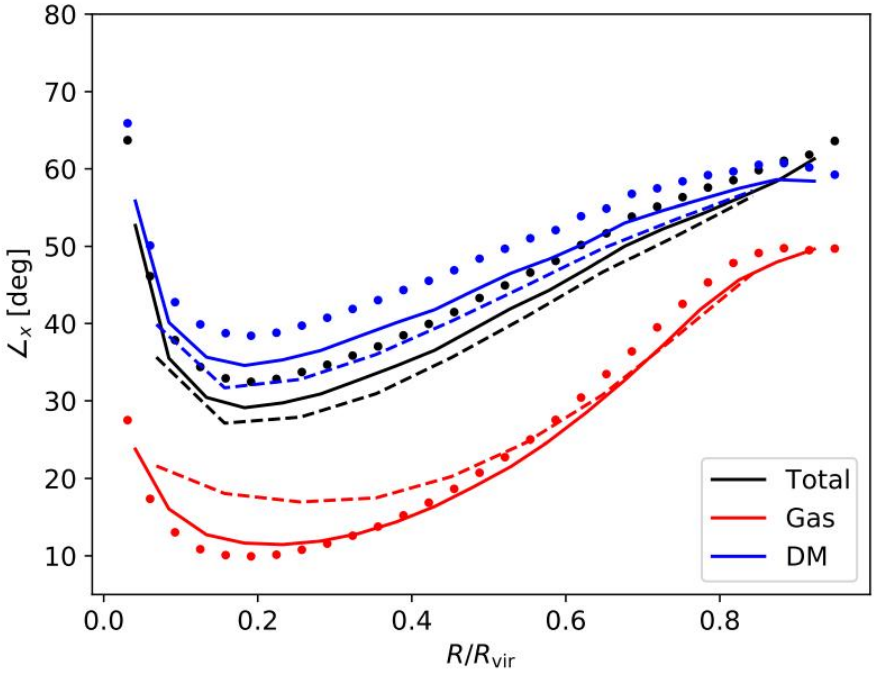

Figure 5. Angle between the spin vectors in adjacent spherical shells. The larger of the angle, the more misaligned a component is with itself. Black, red, blue represent total components, gas and DM respectively. Dashed, solid and dotted lines represent the haloes binned into 10, 20, and 30 bins, respectively.

3 CONTROL SIMULATIONS

No.	$a_x : a_y : a_z$	λ	κ	c	Δc	$j_{\rm gas,ini}$	$j_{\rm gas,fin}$	$j_{\rm DM,ini}$	$j_{\rm DM,fin}$	$j_{\rm gas}/j_{\rm DM}$	$\Delta(j_{\rm gas}/j_{\rm DM})$	$\Delta\lambda$
1	1.0:1.0:1.0	0.03	0.20	3.108	0.015	1288	1287	1288	1288	1.00	0.002	0.00000
2	1.0:1.0:1.0	0.06	0.20	2.937	0.010	2586	2587	2586	2587	1.00	0.002	0.00000
3	1.0:1.0:1.8	0.03	0.20	2.774	0.024	1289	1290	1289	1289	1.00	0.001	0.00000
4	1.0:1.0:1.8	0.06	0.20	2.673	0.012	2594	2594	2594	2594	1.00	0.000	0.00000
5	1.2:1.0:1.2	0.03	0.20	3.031	0.015	1288	1317	1288	1283	1.03	0.003	0.00011
6	1.2:1.0:1.2	0.06	0.20	2.854	0.007	2587	2656	2587	2575	1.03	0.006	0.00027
7	1.4:1.0:1.4	0.03	0.20	2.903	0.020	1288	1353	1288	1275	1.06	0.016	0.00026
8	1.4:1.0:1.4	0.06	0.20	2.805	0.007	2587	2737	2587	2557	1.07	0.017	0.00059
9	1.6:1.0:1.6	0.03	0.20	2.876	0.015	1292	1381	1292	1274	1.08	0.029	0.00035
10	1.6:1.0:1.6	0.06	0.20	2.834	0.012	2594	2817	2594	2549	1.11	0.012	0.00087
11	1.8:1.0:1.8	0.03	0.20	2.912	0.015	1301	1391	1301	1283	1.08	0.027	0.00035
12	1.8:1.0:1.8	0.06	0.20	2.913	0.018	2614	2901	2614	2553	1.14	0.014	0.00113
13	2.0:1.0:2.0	0.03	0.20	2.962	0.011	1313	1427	1313	1289	1.11	0.031	0.00044
14	2.0:1.0:2.0	0.06	0.20	2.975	0.004	2637	2954	2638	2570	1.15	0.016	0.00123
15	1.2:1.0:1.0	0.03	0.20	2.979	0.016	1288	1336	1288	1278	1.05	0.014	0.00019
16	1.2:1.0:1.0	0.06	0.20	2.827	0.015	2586	2692	2586	2566	1.05	0.009	0.00041
17	1.4:1.0:1.0	0.03	0.20	2.794	0.005	1288	1527	1289	1240	1.23	0.034	0.00094
18	1.4:1.0:1.0	0.06	0.20	2.797	0.009	2586	3148	2586	2473	1.27	0.025	0.00221
19	1.6:1.0:1.0	0.03	0.20	2.819	0.015	1287	1630	1288	1219	1.34	0.043	0.00135
20	1.6:1.0:1.0	0.06	0.20	2.766	0.010	2583	3480	2584	2403	1.45	0.010	0.00353
21	1.8:1.0:1.0	0.02	0.20	2.748	0.014	858	1132	858	803	1.41	0.107	0.00108
22	1.8:1.0:1.0	0.03	0.15	3.218	0.041	1278	1731	1278	1186	1.46	0.010	0.00181
23	1.8:1.0:1.0	0.03	0.20	2.739	0.020	1288	1690	1288	1207	1.40	0.033	0.00159
24	1.8:1.0:1.0	0.03	0.25	2.201	0.007	1300	1553	1300	1249	1.24	0.041	0.00099
25	1.8:1.0:1.0	0.04	0.20	2.706	0.003	1718	2385	1718	1585	1.51	0.042	0.00263
26	1.8:1.0:1.0	0.06	0.20	2.591	0.003	2583	3711	2583	2355	1.58	0.043	0.00444
27	1.8:1.0:1.0	0.08	0.20	2.471	0.003	3453	5006	3454	3140	1.59	0.059	0.00610
28	1.8:1.0:1.0	0.10	0.20	2.394	0.006	4333	6077	4333	3980	1.53	0.017	0.00683
29	1.8:1.8:1.0	0.03	0.20	2.923	0.008	1301	1301	1301	1300	1.00	0.001	0.00000
30	1.8:1.8:1.0	0.06	0.20	2.926	0.008	2608	2612	2608	2609	1.00	0.001	0.00001
31	2.0:1.0:1.0	0.03	0.20	2.588	0.014	1288	1713	1288	1203	1.42	0.048	0.00168
32	2.0:1.0:1.0	0.06	0.20	2.495	0.007	2583	3661	2583	2365	1.55	0.031	0.00425

Table 2. Initial conditions and results of sAM of all the control simulations. All the haloes rotate along z axis. Column (1): Simulation number; (2) the $a_x : a_y : a_z$ ratio of the spherical/elliptical (proto-)haloes (3) Initial Peebles spin parameter; (4) velocity dispersion factor; (5) collapse factor defined as equation 12; (6) standard deviation of collapse factor; (7) sAM of gas in the initial condition; (8) sAM of gas in the final snapshot; (9) sAM of DM in the initial condition; (10) sAM of DM in the final snapshot; (11) ratio of sAM of gas to DM; (12) standard deviation of sAM ratio. (13) spin transfer parameter $\Delta\lambda$, defined as equation 10.

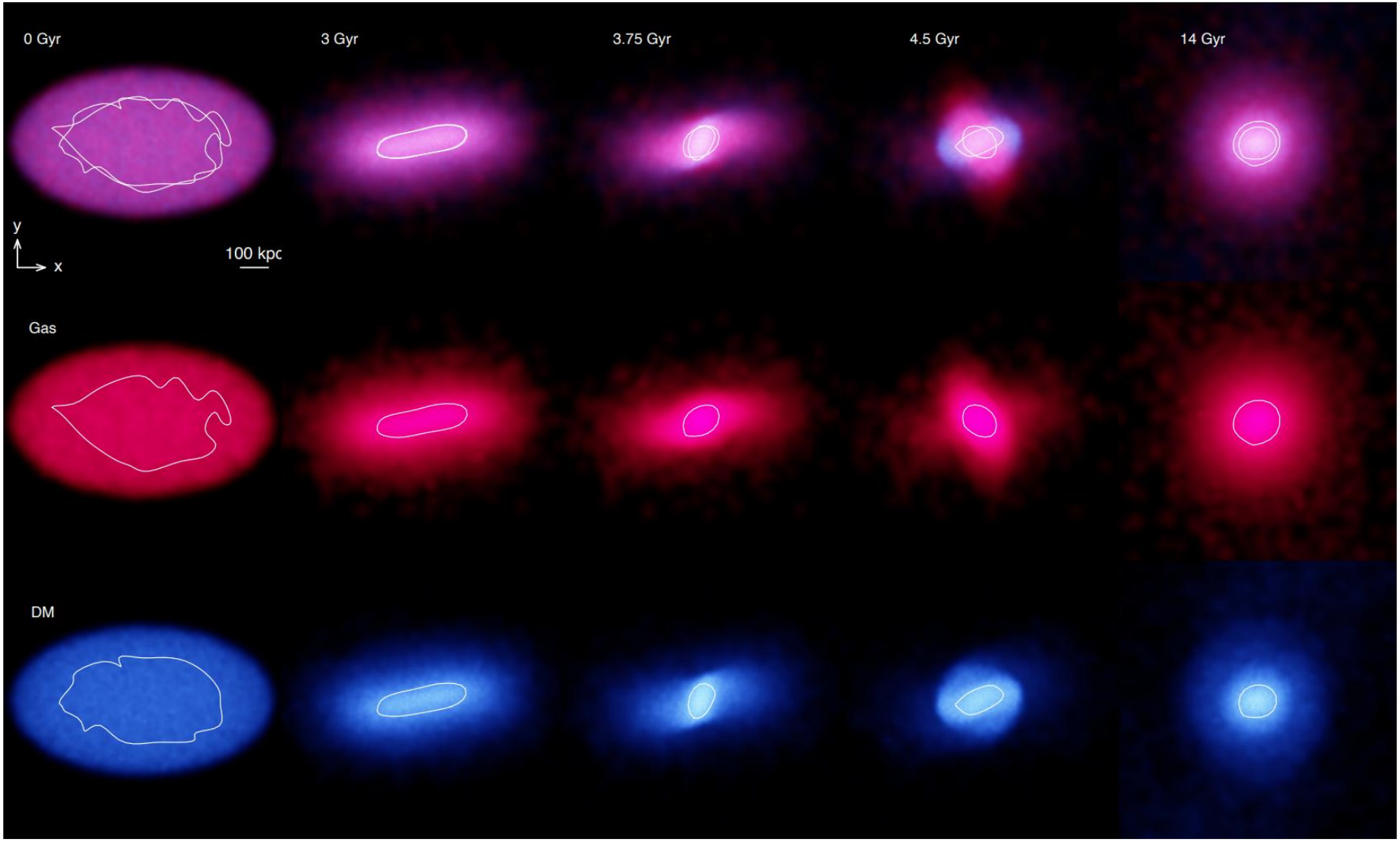

Figure 7. Five snapshots of a prolate halo rotating counterclockwise in the xy-plane. The set up of this halo is shown in Table 2 No.26. Each column from left to right represents the snapshot in 0, 3, 3.75, 4.5 and 14 Gyr, respectively. Each line from top to bottom represents total components, gas and DM respectively. The white contours include 50% materials within it.

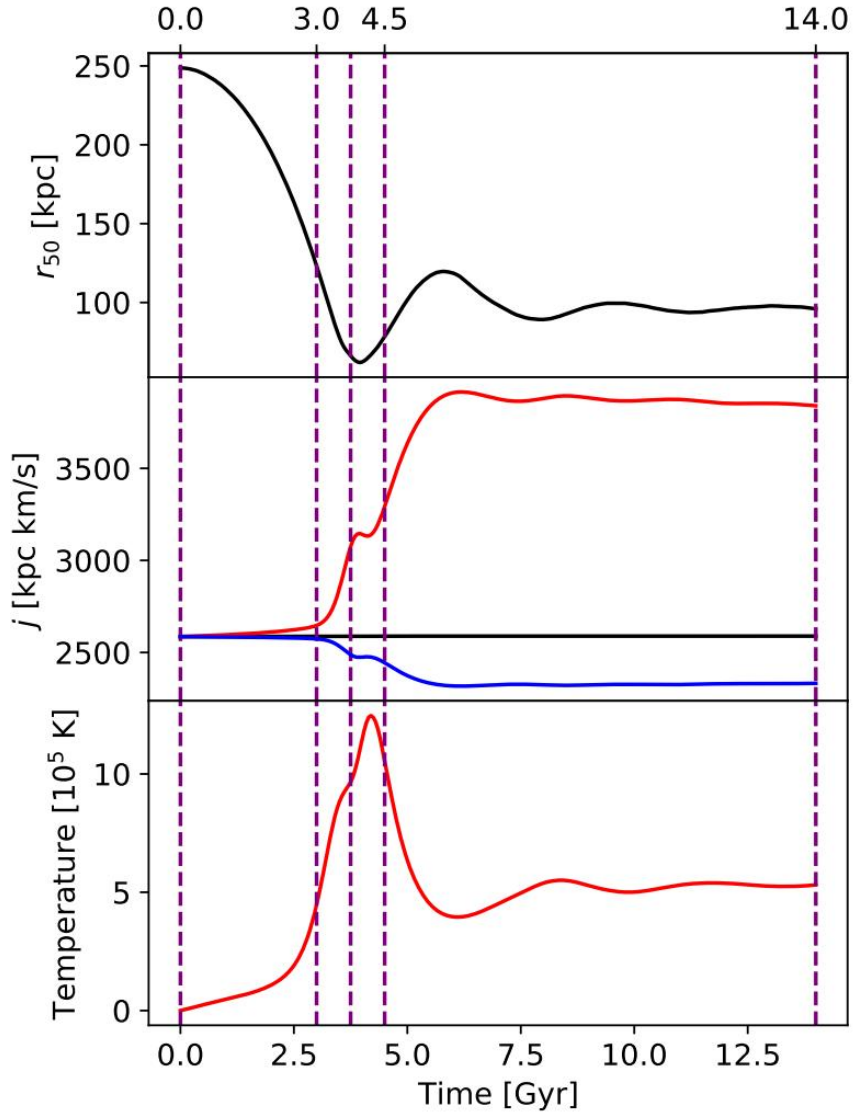

$$\Delta\lambda = \frac{\Delta J|E|^{1/2}}{GM^{5/2}}. \tag{10}$$

$$g = \frac{a_x^2 - a_y^2}{a_z^2}, \tag{11}$$

$$c = \frac{r_{50}(t_i)}{r_{50}(t_f)}, \tag{12}$$

$$\lambda = \frac{J|E|^{1/2}}{GM^{5/2}}, \tag{1}$$

Figure 8. *Top panel*: Half mass radius evolution of the halo. *Middle panel*: sAM evolution of total components (black), gas (red) and DM (blue), respectively. *Bottom panel*: gas temperature evolution of the halo gas. Five purple dashed lines show the positions of five snapshots in Figure 7.

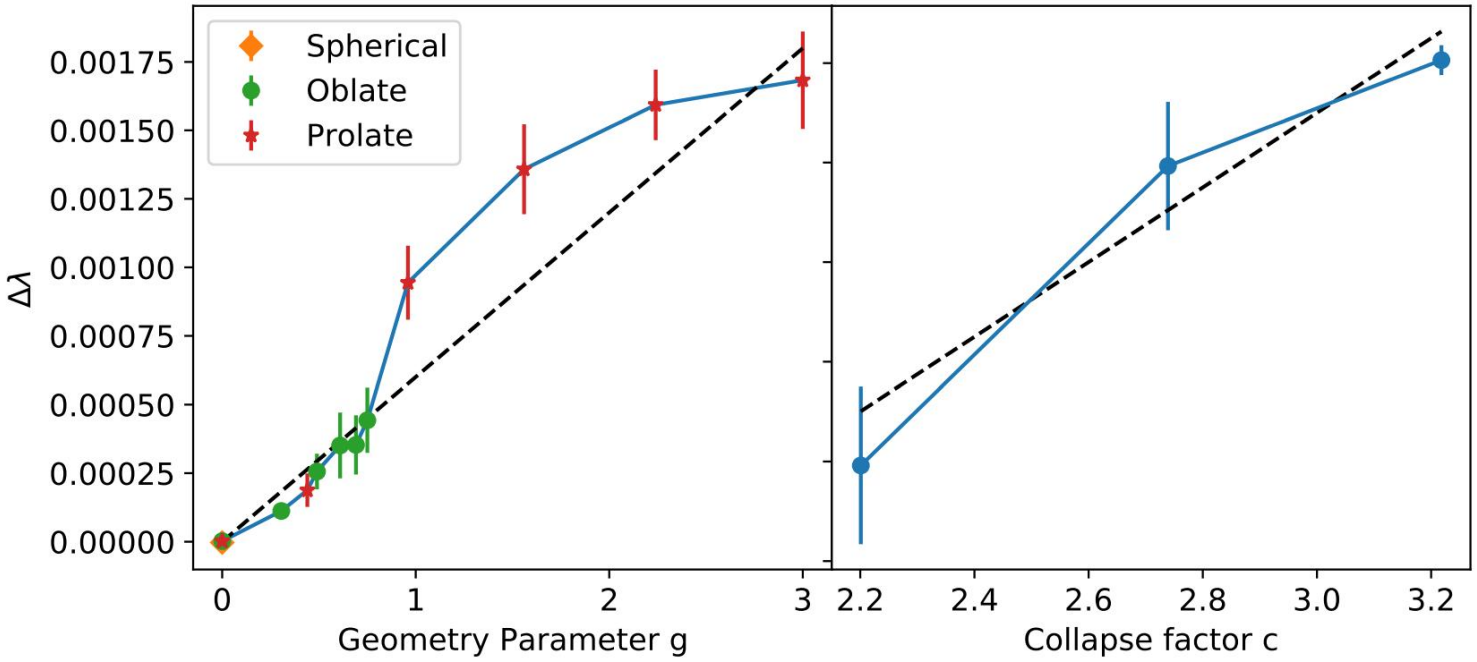

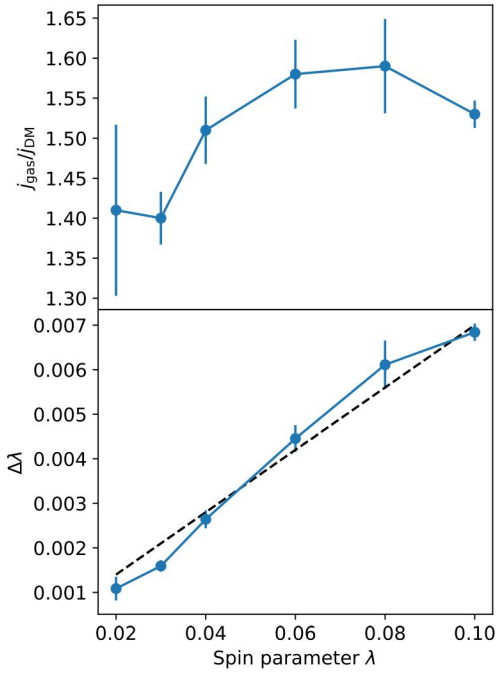

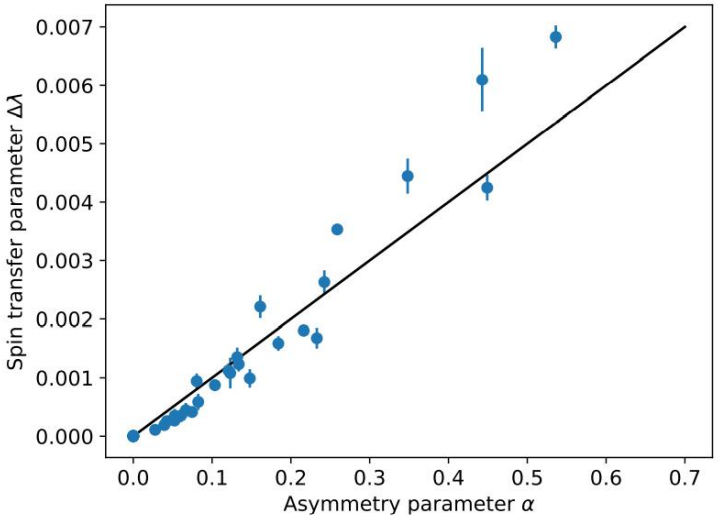

$$\alpha - g\,\lambda\,c - \frac{a_x^2 - a_y^2}{a_z^2} \times \lambda \times \frac{r_{50}(t_i)}{r_{50}(t_f)}. \tag{13}$$

We then fit the linear model

$$\Delta\lambda = k\alpha \tag{14}$$

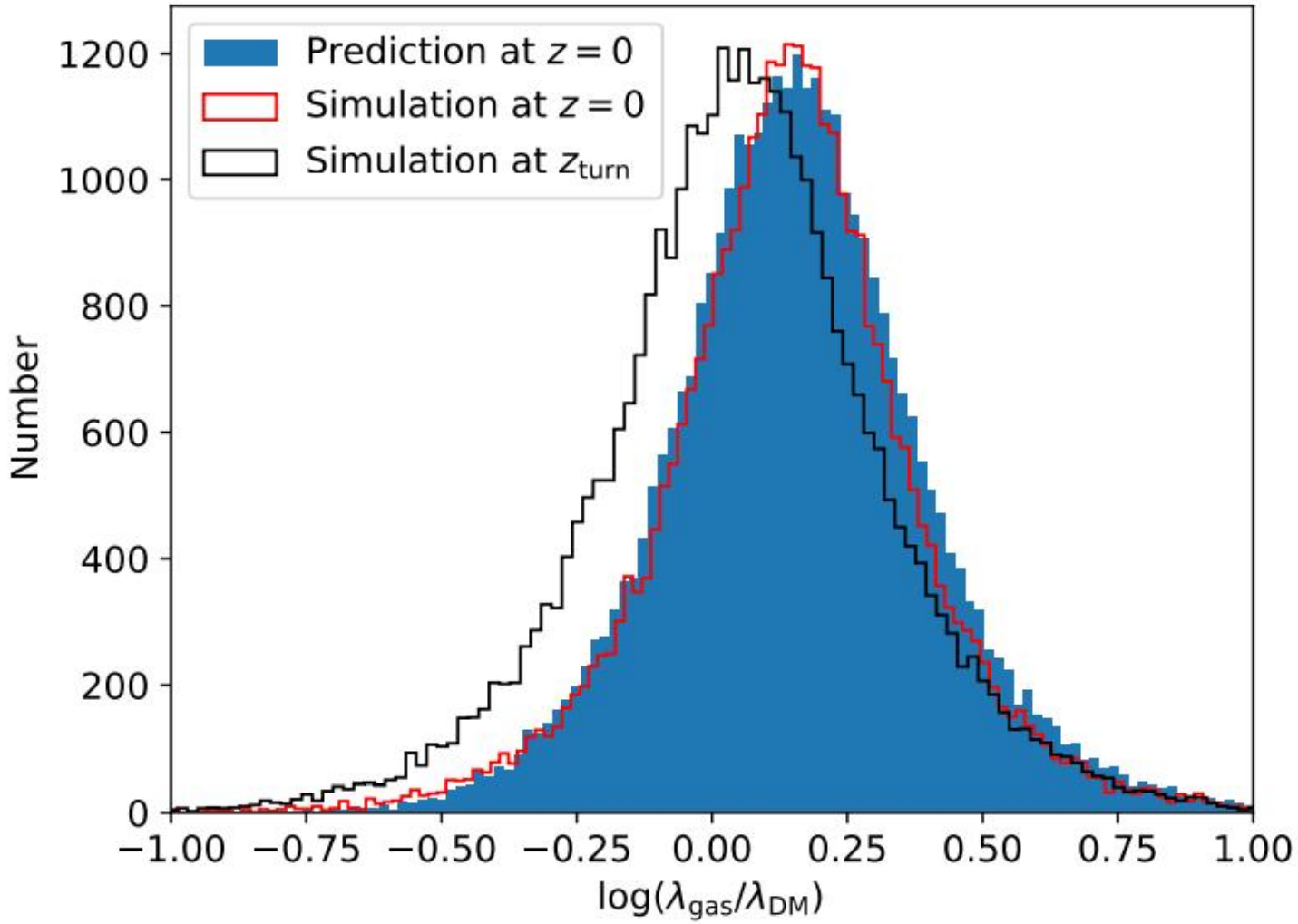

Figure 13. Blue shows the distribution of $\lambda_{\rm gas}/\lambda_{\rm DM}$ predicted by equation 23 from SURFS. This distribution is very similar to the true distribution (red line).